Direct imaging of optical interference in erbium-doped Al2O3 waveguides

Direct imaging of optical interference in erbium-doped Al_2O_3 waveguides

G. N. van den Hoven and A. Polman

FOM-Institute for Atomic and Molecular Physics, Kruislaan 407, 1098 SJ Amsterdam, The Netherlands

C. van Dam, J. W. M. van Uffelen, and M. K. Smit

Department of Electrical Engineering, Delft University of Technology, Mekelweg 4, 2628 CD Delft, The Netherlands

Received November 7, 1995

Interference of 1.48-μm light in multimode interference waveguides is made visible by imaging green and infrared upconversion luminescence from Er^{3+} ions dispersed in the waveguide. A two-dimensional mode density image can be derived from the data and agrees well with mode calculations for this structure. This new technique provides an interesting tool for the study of optical mode distributions in complicated waveguide structures and photonic band-gap materials.

PACS numbers: 42.30.Yc, 78.55.Hz, 42.82.Et, 42.25.Bs.

Light confined in optical waveguides or in more complex integrated optic devices can exist in a finite number of well-defined modes that interfere with one another, leading to characteristic optical intensity distributions. Knowledge of these mode densities is essential for the design and fabrication of integrated optical structures. In wavelength-scale structures such as photonic band-gap materials and optical cavities, the optical mode density determines the spontaneous emission rate of luminescent transitions.[1,2] In many cases, the optical mode density or photonic band structure can be calculated from Maxwell's equations; here we show how two-dimensional optical mode intensity distributions in optical waveguides can be determined experimentally.

Direct imaging of the light-intensity distribution in a waveguide is difficult, as the light propagates along the waveguide and only a small fraction of the intensity is scattered in other directions. Imaging of this scattered light is possible, but because scattering occurs at inhomogeneities in the waveguide, the scattered light does not directly relate to the intensity distribution. Other method for studying intensity distributions in waveguides, such as imaging of the cleaved end faces of the waveguide, give only the field intensity distribution at the end face and have a destructive effect on the waveguide.

In this study we use upconversion luminescence from Er^{3+} ions dispersed in a waveguide to probe the light-intensity distribution. Er^{3+} is an optical dopant, which exhibits sharp luminescent transitions when incorporated in a solid host.[3] The Er^{3+} energy-level diagram is shown schematically in Fig. 1. Er^{3+} ions can be excited to their first excited level [$^4I_{13/2}$; Fig. 1(a)] when 1.5-μm pump light is launched into the waveguide. At high pump intensities, a high concentration of excited Er^{3+} ions is obtained, which can interact through a cooperative upconversion process: one excited ion transfers its excitation energy to another, promoting the latter to a higher-lying energy level [$^4I_{9/2}$; Fig. 1(b)]. This leads to the buildup of population in the second excited state [$^4I_{11/2}$; Fig. 1(b)] and to luminescence at 980 nm. If the pump intensity is high enough, a high concentration of ions in this second excited state is reached, and a second cooperative upconversion event involving two ions in this state can occur, resulting in excitation of even higher energy levels [$^2H_{11/2}$ and $^4S_{3/2}$; Fig. 1(c)]. This two-step upconversion process leads to green luminescence emission around 520 and 545 nm, with an effective peak wavelength of 540 nm. Details of cooperative upconversion and its dependence on the light intensity in Er-implanted Al_2O_3 waveguides can be found in Ref. 4. By imaging the isotropically emitted 540- or 980-nm luminescence from the Er^{3+} ions, one can measure the intensity distribution, and therefore the optical modes, of the 1.48-μm pump light in the waveguide. We use a multimode interference (MMI) coupler structure to study optical mode densities. The device consists of an optical waveguide section that supports 12 optical modes. Because the different modes propagate at

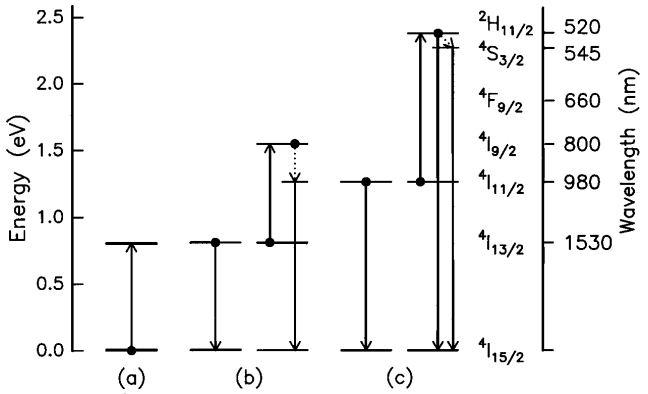

Fig. 1. Er^{3+} energy-level diagram showing (a) excitation of Er^{3+} by absorption of a 1.48-μm photon, (b) cooperative upconversion from the first excited state, giving rise to emission at 980 nm, and (c) cooperative upconversion from the second excited state, giving rise to emission around 540 nm.

0146-9592/96/080576-03$10.00/0

different phase velocities, phase shifts between the modes occur, leading to interference. An interesting feature of MMI is its self-imaging property: at certain positions in the waveguide single or multiple images of the input intensity distribution are reproduced. Self-imaging and other interference effects are applied in many integrated optical devices for the routing, splitting, switching, and multiplexing of light.[5–9]

We used radio-frequency magnetron sputter deposition to deposit a 600-nm-thick Al_2O_3 waveguide film upon a thermally oxidized Si(100) substrate. The deposition parameters are reported in Refs. 10 and 11. The Al_2O_3 film was doped with Er with 1.3-MeV Er ion implantation, with the sample held at 77 K during the implant. The Er fluence was 1.62×10^{16} Er/cm^2. The Er implantation profile has a Gaussian shape and is peaked at a depth of 270 nm, with a full width at half-maximum of 160 nm, as confirmed by Rutherford backscattering spectrometry measurements. The Er peak concentration is 1.4 at. %.

A 21-μm-wide MMI section, center fed by a 2-μm-wide input waveguide was defined with photolithography. An Ar atom beam was used to etch 300 nm of the Al_2O_3 film, resulting in ridge waveguides under the previously defined areas. Following this, a top SiO_2 cladding layer was sputter deposited. Figure 2 is a schematic of the MMI structure. The sample was annealed at 825 °C for 1 h, which is known to result in low-loss waveguides ($\approx$0.4 dB/cm) (Ref. 11), and is necessary to activate the Er optically.[12] Last, the samples were saw cut to $\approx$9 mm in length, and the end faces were mechanically polished in order to attain optimal light coupling into the waveguide.

Approximately 5 mW of 1.48-μm light from a Philips InGaAsP diode laser was coupled into the waveguide by the use of a tapered optical fiber. The luminescence emission from the waveguide was imaged with an optical microscope that was mounted normal to the sample surface (x dimension in Fig. 2). A Philips LDH 0805 CCD camera was placed on top of the microscope. With the camera both visible color and infrared monochrome images could be made. Filters were used to ensure that only the wavelengths of interest were detected by the camera. A frame grabber was used to store images for further analysis.

Plate I(a) shows a two-dimensional image of the 21-μm-wide Er-doped Al_2O_3 MMI waveguide section pumped with 1.48-μm laser light. The image is clearly visible to the eye, and the emission spectrum peaks in the green at 540 nm. A distinct interference pattern is observed, because of the interference of the different optical modes in the waveguide.

The interference images shown in Plate I(a) can be understood by solution of Maxwell's equations under the boundary conditions imposed on the light field by the waveguide. We consider the problem in only the lateral dimension (in plane; y direction); the equations for the transversal field (x direction) can be solved independently and show a single mode in this dimension. Considering only transverse-electric modes (transverse-magnetic modes show essentially the same behavior), we note that solutions to the wave equation for the electric field are of the form

$$E(x, y, z, t) = \tfrac{1}{2}E(y)\{\exp[i(\omega t - \beta z)] + \text{c.c.}\}, \quad (1)$$

where x, y, and z are the directions as shown in Fig. 2, t is time, ω is the angular frequency of the light, β is the z component of the wave vector, and c.c. is the complex conjugate. Solutions to $E(y)$ may be obtained by substitution of Eq. (1) into the wave equation; each solution corresponds to an allowed optical mode in the waveguide. These modes can be either cosine (even) or sine (odd) functions of y inside the core of the waveguide, with exponentially decaying tails outside.

The 21-μm-wide MMI section in Fig. 2 has effective indices of refraction $n = 1.534$ for the core and $n = 1.480$ for the cladding. This waveguide supports six even and six odd modes. Only the even modes need to be considered, as the MMI waveguide section is symmetrically fed by the input waveguide. Because each mode travels through the waveguide at a different velocity, characterized by its value of β, interference between the modes occurs.

Plate I(b) shows a calculation of the interference mode pattern, converted to Er luminescence intensity by taking into account the nonlinear dependence of the upconversion emission with pump power in the waveguide.[4] Good agreement between the measurements and calculations is observed. In particular, the self-imaging principle is demonstrated, where an N-fold image of the input light field is obtained at a distance L that satisfies[9]

$$L = (3L_\pi/4)/N, \quad (2)$$

where L_π is the beat length between the 0th- and 1st-order modes in the MMI section [$L_\pi = \pi/(\beta_0 - \beta_1)$] and is equal to 685 μm for this particular waveguide. The arrows in Plate I indicate the positions of the input (1) and the positions of 2-, 3-, and 4-fold images of the input light field according to Eq. (2).

A quantitative comparison of the measured interference patterns and the calculations is shown in Fig. 3. Line scans were taken through the measured intensity distributions (in the y direction) both for the green image in Plate I(a) and for a similar measurement made for the 980-nm emission. The line scans were taken at $z = 0$, 257, 171, and 128 μm, corresponding to the positions showing 1, 2, 3, and 4 maxima, respectively, as indicated in Plate I by the arrows. Figure 3 shows these line scans (dots)

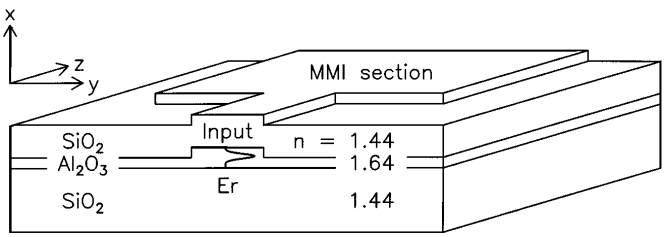

Fig. 2. Schematic of an Er-implanted Al_2O_3 MMI waveguide. The 21-μm-wide multimode section is center fed by a 2-μm-wide input waveguide. The refractive indices n of the layers are indicated together with the Er depth profile.

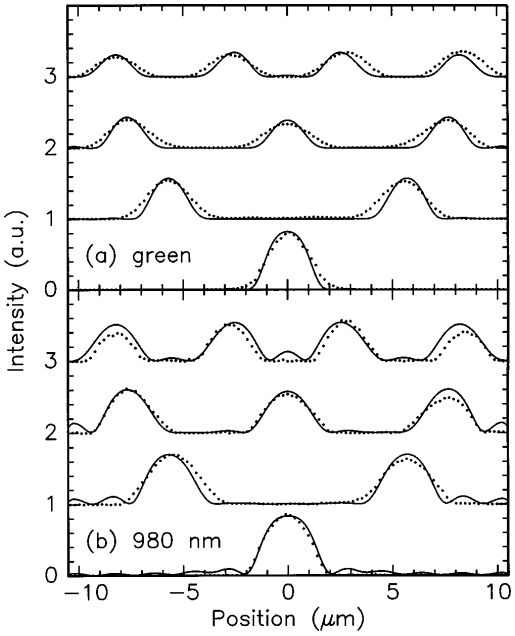

Fig. 3. Line scans of the luminescence intensity around (a) 540 nm and (b) 980 nm (all shown as dots), measured at positions in the waveguide showing 1, 2, 3, and 4 maxima (arrows in Plate I). Calculations of the luminescence intensities are shown as solid curves.

together with calculations of these scans (solid curves). In these calculations, first the input light field was determined by calculation of the overlap between the (calculated) light field imposed by the input waveguide and the six even modes in the MMI section. Because higher-order (radiative) modes were neglected, this leads to sidelobes in the calculation that are not observed experimentally. Second, the higher-order maxima were calculated from the input profile with Eq. (1). Good agreement between the measurements and the calculations is observed.

Note that the technique of using upconversion luminescence allows, in principle, for probing the 1.48-μm mode intensity in the waveguide at the diffraction limit of the luminescence light. For the 540-nm green light used here, this means the measuring resolution is $\sim$3 times better than if the 1.48-μm pump light propagating in the waveguide were imaged directly.

In conclusion, two-dimensional optical mode densities in waveguides are measured with the cooperative upconversion luminescence of Er^{3+} ions as a probe. This new technique for imaging intensity distributions is demonstrated by visualization of multimode interference (MMI) in a MMI coupler. Interference images can be seen both in the visible (540 nm) and in the infrared (980 nm) and match very well to mode calculations. Quantitative agreement between measurement and calculation is obtained for cross sections through the intensity distributions at specific points in the waveguide. This technique can be applied to study many physical phenomena that depend on the shape or density of optical modes, for instance, in complicated waveguide structures and photonic bandgap materials. Furthermore, the use of upconversion luminescence in principle enables one to determine mode densities at a resolution better than the diffraction limit for the propagating light.

The authors thank R. J. I. M. Koper for mechanical polishing of the waveguides and M. H. J. Hagen for help during the experiments. M. L. Brongersma is thanked for stimulating discussions and A. Lagendijk for critical reading of the manuscript. B. H. Verbeek of the Philips Optoelectronic Center is thanked for supplying the high-power InGaAsP 1.48-μm pump laser. This research is part of the research program of FOM and was made possible by financial support from the Dutch Organization for Scientific Research (NWO), the Innovative Research Program (IOP) of the Ministry of Economic Affairs, and the Dutch Technology Foundation (STW).

References

1. E. Yablonovitch, J. Opt. Soc. Am. B **11,** 283 (1993).
2. E. Snoeks, A. Lagendijk, and A. Polman, Phys. Rev. Lett. **74,** 2459 (1995).
3. S. Hüfner, *Optical Spectra of Transparent Rare-Earth Compounds* (Academic, New York, 1980).
4. G. N. van den Hoven, E. Snoeks, A. Polman, C. van Dam, J. W. M. van Uffelen, and M. K. Smit, J. Appl. Phys. **79,** 1258 (1996).
5. E. C. M. Pennings, R. J. Deri, A. Scherer, R. Bhat, T. R. Hayes, N. C. Andreadakis, M. K. Smit, L. B. Soldano, and R. J. Hawkins, Appl. Phys. Lett. **59,** 1926 (1991).
6. R. Adar, C. H. Henry, R. F. Kazarinov, R. C. Kistler, and G. R. Weber, J. Lightwave Technol. **10,** 46 (1992).
7. R. M. Jenkins, J. M. Heaton, D. R. Wight, J. T. Parker, J. C. H. Birbeck, G. W. Smith, and K. P. Hilton, Appl. Phys. Lett. **64,** 684 (1994).
8. M. Bachmann, P. A. Besse, and H. Melchoir, Appl. Opt. **33,** 3905 (1994).
9. L. B. Soldano and E. C. M. Pennings, J. Lightwave Technol. **13,** 615 (1995), and references therein.
10. M. K. Smit, G. A. Acket, and C. J. van der Laan, Thin Solid Films Electron. Opt. **138,** 171 (1986).
11. M. K. Smit, "Integrated optics in silicon-based aluminium oxide," Ph.D. dissertation (Optics Laboratory, Department of Applied Physics, Delft University of Technology, Delft, The Netherlands, 1991).
12. G. N. van den Hoven, E. Snoeks, A. Polman, J. W. M. van Uffelen, Y. S. Oei, and M. K. Smit, Appl. Phys. Lett. **62,** 3065 (1993).